Article

JOURNAL OF COMPOSITE MATERIALS

Journal of Composite Materials
0(0) 1–9

DOI: 10.1177/0021998318825295
journals.sagepub.com/home/jcm
SAGE

A closed-form solution for the barrier properties of randomly oriented high aspect ratio flake composites

A Tsiantis[1] and TD Papathanasiou[1,2]

Abstract

We derive closed-form solutions for the barrier factor of flake-filled composites, in which the flakes are randomly placed and oriented, with the orientation angles uniformly distributed in an interval $[-\varepsilon, +\varepsilon]$, $0 < \varepsilon < \pi/2$. Our solutions are based on the arithmetic and harmonic averaging of the diffusivity of unidirectional misaligned flake systems. Using large-scale 2D simulations, some involving up to 50,000 individual flakes in one unit cell and spanning the regime from dilute to highly concentrated, the proposed solutions are tested against and confirmed by computational results. We use both, traditional 2D and also 1D representations of the flake cross sections. The 1D representation is suitable for very high aspect ratio flakes, such as exfoliated nano-platelets and allows us to model flake nano-composites ($\alpha > 1000$) in which ($\alpha\varphi$) can reach levels in excess of 100. Comparison of the derived closed-form solutions to computational results reveals that both the harmonic and the arithmetic averages are adequate in dilute systems; however, at large values of ($\alpha\varphi$) and (ε), only the harmonic average is in good agreement with the computational results. The predictions of the proposed solution are also compared to those of existing literature models for the effective diffusivity of flake composites. We find that discrepancies become very significant at large (ε) and also at large values of ($\alpha\varphi$), pointing further to the conclusion that the proposed solution is currently the only accurate one to predict the effective diffusivity of randomly oriented and highly concentrated nano-flake composites.

Keywords

Barrier properties, flake composites, orientation

Introduction

Prediction of the barrier properties of flake-filled composites has been the subject of active research in recent years, due to their importance as barrier materials and in nanotechnology. Original models for aligned-flake composites have been derived from analysis of simple unit cells corresponding to idealized flake arrangements.[1,2] These have been found to be in good agreement with computation, even in cases when the spatial arrangement of the flakes deviate drastically from regular packing.[3] The key and rather undisputed result concerning aligned systems is that the Barrier Improvement Factor ($\mathrm{BIF} \sim 1/D_{eff}$), D_{eff} being the effective diffusivity of the composite, is a quadratic polynomial of ($\alpha\varphi$), where (α) is the aspect ratio of the flakes and (φ) their volume fraction.[4] When the flake orientations deviate from perfect alignment, the picture is far less clear. When the flakes assume a fixed orientation with respect to the direction of bulk transport,[5] proposed a model capable of reproducing 2D computational results for ($\alpha\varphi$) up to 40. When the flakes assume random orientations within an interval $[-\varepsilon, +\varepsilon]$, numerical results along with an empirical model capable of representing them for ($\alpha\varphi$) up to 15 have been presented in Papathanasiou and Tsiantis.[6] A review of the state of the art along with a new model for the barrier properties of flake systems in which the flakes orientations are normally distributed within an interval and for ($\alpha\varphi$) up to 5, have been presented in

[1]Department of Mechanical Engineering, University of Thessaly, Greece
[2]Department of Chemical and Materials Engineering, Nazarbayev University, Kazakhstan

Corresponding author:
T.D. Papathanasiou.
Emails: athanasios.papathanasiou@nu.edu.kz; athpapathan@mie.uth.gr

Dondero et al.[7] This problem has also been reviewed in Zid et al.[8] where detailed reference to earlier work has been made. Three-dimensional simulations using the Lattice-Boltzmann method have been presented in Roding et al.[9] and the conclusion was reached that for flakes of high aspect ratio (argued in Roding et al.[9] to be between 4500 and 10,500 for graphene) existing models do not capture the variation of barrier properties. From a literature review, it is evident that, while the topic has received significant attention in the last 15 years, there does not exist a single predictive model capable of capturing both, the effect of concentration and the effect of orientational randomness on the barrier properties of flake composites. This is particularly true for nanocomposites, in which, due to the high (α) very high values of ($\alpha\varphi$) can be achieved; the ($\alpha\varphi$) implied in Roding et al.[9] for graphene–Polyethylene composite can be as high as 100. Since earlier models have been validated with computational results for ($\alpha\varphi$) only up to 7, their suitability for this class of materials is not proven.[9] It is also evident that existing models are based on the ad hoc utilization of orientational metrics without a solid theoretical footing and without preserving the rotational invariance of the diffusivity tensor. With these in mind, the purpose of the present communication is to propose a model for the barrier properties of randomly oriented flake composites which will incorporate both, the effect of flake concentration and the effect of orientational randomness. The model is free of ad hoc pronouncements and is based on averaging of the diffusivity tensor. The model is tested extensively with computational results and is found to be valid for all states of misalignment and for the entire range of ($\alpha\varphi$) that is achievable computationally.

Theoretical

Consider a system of randomly placed and randomly oriented flakes. The orientation of each flake is defined by the angle (θ) formed between the vertical axis (y), which is taken to be the direction of macroscopic diffusion, and the outward normal vector on the flake surface. The horizontal axis is indicated as (x). D_{11} is the diffusivity of such a system of flakes when $\theta = 0^\circ$ (all flakes oriented perpendicular to the direction of macroscopic diffusion) and D_{22} the diffusivity when $\theta = 90^\circ$ (all flakes oriented parallel to the direction of diffusion)—D_{11} and D_{22} are the principal values of the two-dimensional diffusivity tensor, **D**. In this case, the effective diffusivity (D_{eff}) in the direction (y) of such a system of misaligned flakes can be expressed as a function of the misaligned angle (θ) as

$$D_{eff}(\theta) = D_{11}\cos^2(\theta) + D_{22}\sin^2(\theta) \tag{1}$$

Equation (1) can be used to determine the diffusion coefficient of a system of misaligned flakes, provided D_{11} and D_{22} are known. In previous work,[5] we investigated computationally the performance of equation (1) and determined that the best agreement with the computational results was obtained when the models of Nielsen[12] and Lape et al.[4] were used for the principal diffusivities, namely $D_{22} = D_0\frac{1-\varphi}{1+\frac{\varphi}{2\alpha}}$ and $D_{11} = \frac{(1-\varphi)}{(1+\alpha\varphi/\lambda)^2}D_0$ respectively, where D_0 is the diffusivity of the matrix material. The parameter (λ) is meant to reflect the tortuous path of the solute around each flake and it was set to $\lambda = 3$ in the original model of Lape et al.[4]; a value of $\lambda = 2.5$ was found to give the best agreement between equation (1) and our 2D computational results and this value has been used throughout this study. Once established, equation (1) can be used as the basis of deriving estimates of the effective diffusivity in systems in which the flakes assume a range of orientations. For that purpose, some type of averaging must be performed.

The arithmetic mean is defined as $D_{eff} = \frac{1}{N}\sum_i^N D_i$, where D_i for $i = 1 \ldots N$ is the diffusivities of the N sub-cells which comprise the geometry of interest. Each sub-cell is characterized by a flake orientation angle (θ_i). The arithmetic mean corresponds to a system in which mass transport is envisaged to occur through resistances in parallel; this assumption is more consistent with a dilute system of flakes, in which, macroscopically, lines of constant concentration will tend to be equally spaced and parallel to one another. For a continuous distribution of flake orientations with $-\varepsilon \le \theta \le +\varepsilon$ it will be

$$\begin{aligned}\left\langle D_{eff}^{a}\right\rangle &= \frac{1}{2\varepsilon}\int_{-\varepsilon}^{\varepsilon}\left(D_{11}\cos^2\theta + D_{22}\sin^2\theta\right)\mathrm{d}\theta \\ &= \frac{1}{2}(D_{11}+D_{22}) + \frac{\sin(2\varepsilon)}{4\varepsilon}(D_{11}-D_{22})\end{aligned} \tag{2}$$

where brackets are used to indicate averaging and the superscript (α) indicates arithmetic mean. In equation (2), the pre-factor ($1/2\varepsilon$) corresponds to flakes being oriented with equal probability at each orientation within the interval $[-\varepsilon, +\varepsilon]$. Other probability functions can also be included in equation (2). In the special case when $\varepsilon = \pi/2$, corresponding to a system in which the flakes assume all possible orientations with equal probability (random orientation), it is

$$D_{eff}^{\alpha} = \frac{1}{2}(D_{11}+D_{22}) \tag{3}$$

In the dilute limit and using dilute-regime models for D_{11} and D_{22},[12] namely $D_{22} = D_0\frac{1-\varphi}{1+\frac{\varphi}{2\alpha}}$ and $D_{11} = D_0\frac{1-\varphi}{1+\frac{\alpha\varphi}{2}}$,

we can derive an explicit expression for the arithmetic mean of a system with random ($\varepsilon = \pi/2$) distribution of orientations, in terms of (φ) and (α).

$$\left\langle D^a_{eff} \right\rangle = \frac{(1-\varphi)(4\alpha+\varphi+\varphi\alpha^2)}{(2\alpha+\varphi)(2+\alpha\varphi)} \cdot D_0 \tag{4}$$

If the model of Lape et al.[4] is used for D_{11}, the arithmetic mean $\langle D^a_{yy} \rangle$ can also be obtained in closed form in terms of (φ), (α), and (λ) from equation (2) as

$$\left\langle D^{\alpha}_{eff} \right\rangle = \frac{(1-\varphi)\left(\lambda^2\varphi + 4\lambda^2\alpha + 4\lambda\varphi\alpha^2 + 2\varphi^2\alpha^3\right)}{2(2\alpha+\varphi)(\lambda+\alpha\varphi)^2} \tag{5}$$

Equation (5) is also suitable for concentrated systems.

If transport in a flake composite is better approximated by resistances in series, the Harmonic mean, defined as $\frac{1}{D_{eff}} = \frac{1}{N}\sum_1^N \frac{1}{D_i}$, is a more appropriate measure. As above, for a continuous distribution of orientations, it will be

$$\begin{aligned} \left\langle D^h_{eff} \right\rangle^{-1} &= \frac{1}{2\varepsilon}\int_{-\varepsilon}^{\varepsilon} \left(D_{11}\cos^2\theta + D_{22}\sin^2\theta\right)^{-1} \mathrm{d}\theta \\ &= \frac{1}{\varepsilon\sqrt{D_{11}D_{22}}} \cdot \arctan\left[\sqrt{\frac{D_{22}}{D_{11}}}\tan(\varepsilon)\right] \end{aligned} \tag{6}$$

where the superscript (h) indicates the harmonic mean. When $\varepsilon = \pi/2$ (randomly oriented system), equation (6) gives

$$\left\langle D^h_{eff} \right\rangle = \sqrt{D_{11}D_{22}} \tag{7}$$

Closed-form expressions in terms of (α), (λ), and (φ) can be obtained by substituting D_{11} and D_{22} in equation (6) with the corresponding models, as was done in the case of the arithmetic mean (equations (4) and (5) above).

According to the Harmonic averaging (equation (7)), the ratio between the effective diffusivity of a system comprised of aligned flakes over the diffusivity of a system comprised of randomly oriented flakes can be found to be

$$\frac{D_{aligned}}{D_{random}} = \sqrt{\frac{D_{11}}{D_{22}}} = \frac{\lambda\sqrt{\left(\alpha^2 + \frac{\alpha\varphi}{2}\right)}}{\alpha(\alpha\varphi+\lambda)} \tag{8}$$

in which the models of Lape et al.[4] and Nielsen[12] were used for D_{11} and D_{22} respectively. Evidently, for very long flakes, equation (8) predicts that this ratio is proportional to $(1/\alpha\varphi)$.

Finally, the geometric mean provides that $D_{eff} = \left(\prod_1^N D_i\right)^{1/N}$ where $\prod$ indicates a product and (N) is again the number of sub-cells comprising the system. In that case, for a continuous distribution of (θ) it will be

$$\left\langle D^g_{eff} \right\rangle = \exp\left[\frac{1}{2\varepsilon}\int_{-\varepsilon}^{\varepsilon} \ln\left(D_{11}\cos^2\theta + D_{22}\sin^2\theta\right)\mathrm{d}\theta\right] \tag{9}$$

where again a uniform distribution of orientations is assumed and the superscript (g) stands for the geometric mean.

In the following, we will validate the proposed models (equations (2), (6), and (9)) by comparing its predictions to computational results. Subsequently, we will compare its predictions to those of existing literature models. Comparison of model predictions to experimental data is a not-so-straightforward matter, since, in order for the comparison to be meaningful, the microstructure of the physical specimens (in terms of placement, dispersion, and orientation of the platelets/flakes) should be comparable to those of the theoretical model (uniformly dispersed flakes, with their orientations uniformly distributed between $[-\varepsilon, +\varepsilon]$). In addition, several physicochemical factors come into play in nanocomposites and as a result, the observed BIFs show a very significant scatter. Wolf et al.[10] have presented a comprehensive summary and analysis of all experimental data published on the topic of barrier properties of nanocomposites (to O_2, CO_2, and H_2O) between 1995 and 2015. It is very instructive to see that almost half the experimental data show that inclusion of nano-fillers results in a decrease of the BIF of the composite. Wolf et al.[10] clearly show that this is because it is very common, when preparing a nanocomposite specimen, to have other factors present, such as formation of high-D interphases, chemical modification of the matrix, formation of agglomerates, particle attrition, etc. Dontero et al.[11] validated the use of diffusion theory and theoretical diffusivity models for platelet-filled composites systems. They conducted diffusion experiments in carefully constructed, specimens which included carefully aligned slender obstacles, and found a good agreement between measured and computed diffusion profiles.

Results and discussion

Computational

We carry out a comprehensive computational evaluation of the above-proposed models, using earlier obtained data[6] as well as results of new computations. All our computations are two-dimensional and as such, are strictly valid for ribbon composites, which are

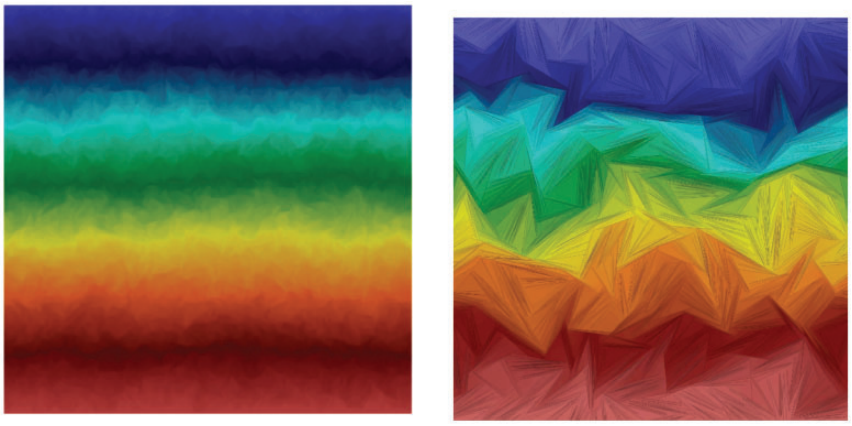

Figure 1. Left: Example geometry and concentration profile in a system containing $N = 50{,}000$ individual flake cross sections with $\alpha\varphi = 10$. Due to their small size, the outline of the flakes is only faintly visible and can be inferred by local variations in the concentration field. Right: Example geometry with $N = 3000$ and $\alpha\varphi = 20$. In both cases, the flakes assume fully random orientations ($\varepsilon = \pi/2$).

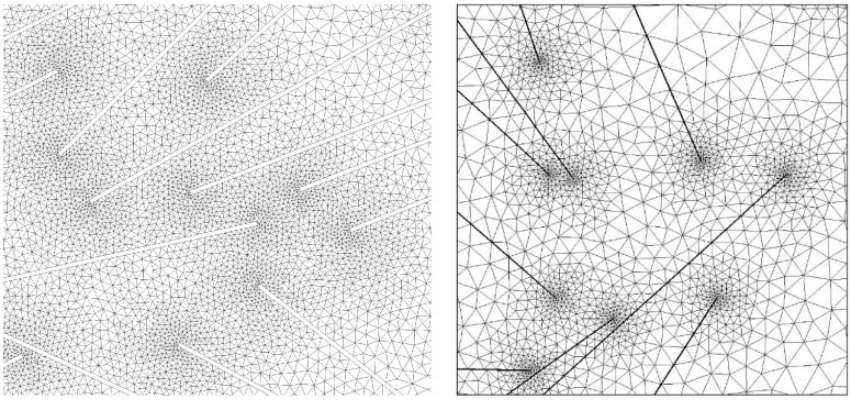

Figure 2. Left: Detail of a geometry and the corresponding computational mesh, when the flake cross sections are represented by 2D rectangles of aspect ratio $\alpha = l/t$. Right: Corresponding detail and mesh when the flakes are represented by one-dimensional lines. (l) and (t) are the length and thickness of the flake respectively.

materials in which the flakes have a very long length in the out-of-plane direction. Comparison between 2D and 3D computational results in randomly oriented flake systems are currently unavailable; however, the 2D results provide a low (conservative) estimate of the BIF of the composite. In all cases, the open-source computational environment OpenFoam was used. Details of the computations have been presented in Tsiantis and Papathanasiou[5] and Papathanasiou and Tsiantis[6] and are omitted here for the sake of brevity. Each geometry (unit cell) contained usually ~ 3000 randomly placed impermeable flake cross sections; however, unit cells containing 10,000 or 50,000 flake cross sections were also considered. Such an example is shown in Figure 1. We look at systems ranging from dilute to concentrated and in which the fiber orientations (θ) assume random values in the interval $[-\varepsilon, +\varepsilon]$, $0 < \varepsilon < \pi/2$.

In addition to two-dimensional flake cross sections, we also consider an alternative, one-dimensional flake representation, suitable for flakes of very high aspect ratio, as would be the case in platelet-reinforced nanocomposites. In this, each flake is represented by one line, on which the impermeability condition ($\partial C/\partial \boldsymbol{n} = 0$) is applied. Figure 2(b) shows a detail of such a geometry containing 1D flake cross sections, along with the computational mesh. For comparison, a 2D representation is shown in Figure 2(a).

Obviously, when impermeable lines are used, instead of rectangles, to represent flake cross sections, the use of the volume fraction (φ) becomes irrelevant. Recognizing that in a 2D representation it is $\alpha\varphi = \frac{Nl^2}{HL}$, where ($l$) is the length of each flake and H, L the dimensions of the containing unit cell, we choose to form "lines" by connecting the two midpoints of the short sides of the corresponding rectangle (Figure 2). In this

case, a measure of the concentration of the corresponding 1D-flake system is the ratio $\left(\frac{Nl^2}{HL}\right)$. Figure 3 shows a comparison between the predictions of the two approaches for D_{eff}. It can be seen that the use of impermeable lines to represent flakes is an acceptable simplification when large aspect ratio flakes are considered. Because of the simplicity an 1D representation affords to meshing, the range of computationally achievable flake concentrations is expanded in this manner. However, since in the 1D representation the excluded volume is always zero, irrespective of the number and size of the flakes, this approach is expected to break down at high values of (φ). This is not a serious shortcoming however; when high aspect ratio flakes are involved, very large ($\alpha\varphi$) values can be achieved at very low values of (φ); with reference to Figure 3, the maximum achieved value of $\alpha\varphi = 30$ corresponds to $\varphi = 0.003$ (0.3%). The good agreement in Figure 3 suggests that, for the loadings and (α) considered, the observed barrier property improvement is due to the increase in the tortuosity caused by the presence of the flakes and not the result of any excluded volume. This conclusion was also reached in Roding et al.[9] and appears to suggest that in flake nanocomposites the improvement in barrier performance is entirely due to the increase of the tortuosity of the medium.

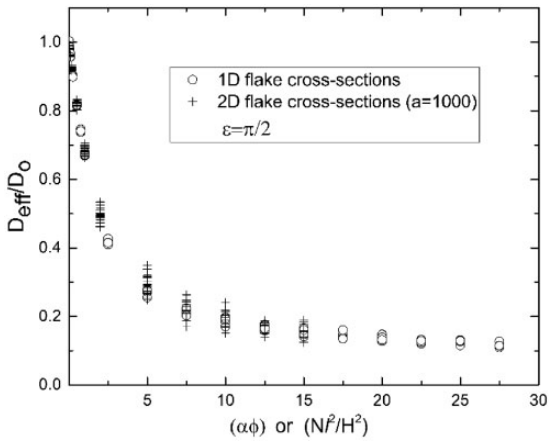

Figure 3. Comparison of the predicted effective diffusivity of a system with randomly oriented flake cross sections ($\varepsilon = \pi/2$) which are considered to be either 2D rectangles of aspect ratio $\alpha = 1000$ or 1D lines, for a range of values of ($\alpha\varphi$) (in the 2D representation) and $\left(\frac{Nl^2}{HL}\right)$ (in the 1D representation). In the case of 2D representation, the data of Papathanasiou and Tsiantis[6] were used (+). In the case of 1D representations, results shown (o) correspond to $N = 3000$.

Comparison of theoretical predictions to computational results

Figure 4 shows a comparison between the Arithmetic, Harmonic, and Geometric averages, defined by equations (2), (6), and (9) above, to the computational results for D_{eff}. As outlined previously, in computing an average one needs to decide on an appropriate model for the principal diffusivities D_{11} and D_{22}. For D_{22}, Nielsen's model[12] has been shown to be reliable in the case when the flakes are aligned parallel to the direction of diffusion even for ($\alpha\varphi$) as high as 50. In the following, we use the model of Lape et al.[4] for D_{11}, as it gave the best fit to earlier computational results,[5,6] with a value of $\lambda = 2.5$.

As expected, it is $\langle D^a_{yy}\rangle \geq \langle D^g_{yy}\rangle \geq \langle D^h_{yy}\rangle$. When the two terms D_{11} and D_{22} in the integral kernel of equations (2), (6), and (9) are approximately equal (as would be the case in a dilute suspension of flakes, $\alpha\varphi < 0.1$) the results of the three averages are practically indistinguishable. However, significant differences appear in the concentrated regime. These differences are more pronounced at higher values of (ε). When these differences become significant (large values of (ε) and ($\alpha\varphi$)), choice of the correct averaging becomes important. It is evident that the arithmetic average is definitely an inappropriate model for computing the effective diffusivity of randomly oriented and concentrated flake

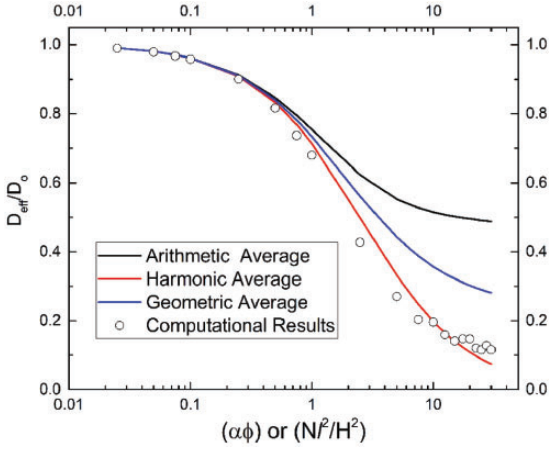

Figure 4. Comparison of computational results (points) and the predictions of the arithmetic, harmonic, and geometric averages (equations (2), (6), and (9)) based on the model of Lape et al.[4] for D_{11} and Nielsen[12] for D_{22}. Random flake orientations ($\varepsilon = \pi/2$). The computational results shown correspond to the use of 1D flake cross sections, therefore, instead of ($\alpha\varphi$) the corresponding measure of concentration is $\frac{Nl^2}{HL}$, where $N = 3000$ and H = L are the dimensions of the unit cell.

systems—irrespective of the models used for D_{11} and D_{22}. In conjunction with the model of Lape et al.,[4] the harmonic average is found to give a very good fit to the computational results for the entire range of ($\alpha\varphi$) studied.

As the spread in flake orientations narrows, the three averages come closer, with the harmonic mean

remaining closer to the computational results, as shown in Figure 5 for $\varepsilon = 0.8$ rad. The generation of computational meshes becomes easier as the flake orientation range decreases; as a result, the computationally achievable range of ($\alpha\varphi$) increases as (ε) decreases.

Comparisons for a case of lower aspect ratio ($\alpha = 50$), in which flake cross sections are necessarily represented as 2D rectangles, are shown in Figure 6. Large values of ($\alpha\varphi$) are not achievable when the flake aspect ratio is low. In the case of Figure 6 with $\alpha = 50$, $\alpha\varphi = 10$ implies a volume fraction of 20%; this level of packing is at the limit of what can be achieved in real composite fabrication as well as in the generation of a computational unit cell.

The analytical predictions for the ratio $D_{aligned}/D_{random}$, expressed by equation (8), are compared to computational results in Figure 7. The implication of this chart as well as of equation (8) is that the ratio of the BIFs of the aligned and random composite scales with ($\alpha\varphi$) and thus, the benefit to be gained by

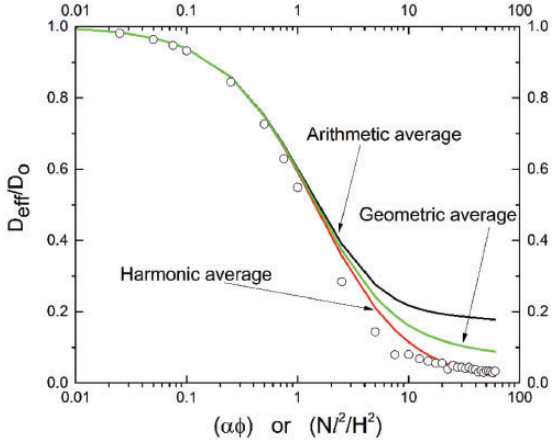

Figure 5. Comparison of computational data (circles) and the predictions of the arithmetic, harmonic, and geometric averages. Random fiber orientation between [$-\varepsilon$, $+\varepsilon$] ($\varepsilon = 0.8$ rad or 45.8°). The computational results shown correspond to the use of 1D flake cross sections, therefore, instead of ($\alpha\varphi$) the corresponding measure of concentration is $\frac{Nl^2}{HL}$, where $N = 3000$, l is the flake length, and H = L are the dimensions of the unit cell.

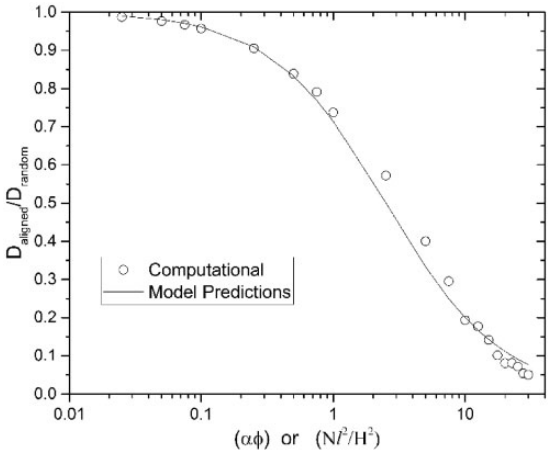

Figure 7. Comparison between analytical predictions based on the proposed model (equation (8), line) and computational results (o). The latter were obtained using 1D representation of the flakes and the former correspond to $\alpha = 1000$. The concentration corresponding to the computational results is expressed by the ratio (Nl^2/H^2), as outlined in previous section.

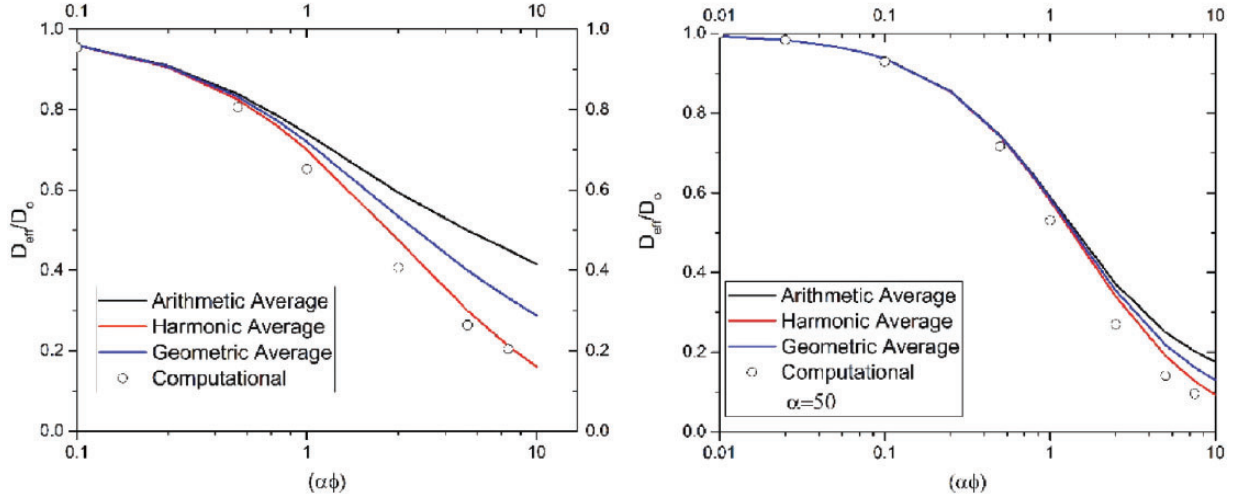

Figure 6. Comparison of computational data (points) corresponding to $\alpha = 50$ and the predictions of the arithmetic, harmonic, and geometric averages. Left: Random fiber orientation ($\varepsilon = \pi/2$); Right: $\varepsilon = 45°$. 2D representation of the flake cross sections.

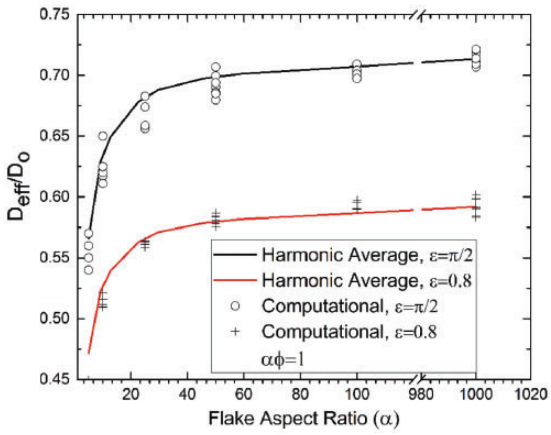

Figure 8. Effect of flake aspect ratio on the D_{eff} as predicted by equation (6) (lines) for $\varepsilon = \pi/2$ and $\varepsilon = 0.8$ rad. In both cases, $\alpha\varphi = 1.0$. Points are computational results obtained for $N = 500$. 2D representation of flake cross sections.

aligning the flakes is larger the more concentrated the system is.

The effect of the flake aspect ratio, as predicted by the Harmonic average (equation (6)), is compared to computational results in Figure 8, for fully random flake orientations ($\varepsilon = \pi/2$) and for $\varepsilon = 0.8$ rad. The numerical data as well as the model predictions follow an asymptotic behavior at increasing (α), with a plateau value already reached at $\alpha = 100$. This is in agreement with earlier published theoretical studies[3,7,13,14] as well as in agreement with experimental studies in well-dispersed nanocomposites.[10]

Comparison with existing models

Among existing models which express the effect of misorientation on the barrier properties of flake composites, the model of Bharadwaj[16] was proposed by combining Nielsen's model[12] with Herman's orientation parameter $H = \frac{1}{2}\left(3\langle\cos^2(\theta)\rangle - 1\right)$ where the brackets $\langle\rangle$ indicate ensemble averaging over the flake population. For general, three-dimensional orientation distributions, the parameter (H) takes the value of zero for a random system, 1 for flakes aligned in the direction from which the angle (θ) is measured (i.e., perpendicular to the direction of diffusion) and -0.5 for flakes oriented along the direction of diffusion. For two-dimensional distributions of orientations, such as those dealt with in this study, this interpretation is no longer correct. In a 3D randomly oriented distribution of flakes it is $\langle\cos^2(\theta)\rangle = 1/3$, while for a 2D random distribution of orientations it is $\langle\cos^2(\theta)\rangle = 1/2$. For this reason, we express the Herman parameter as $H = \frac{1}{2}[2\langle\cos^2(\theta)\rangle - 1]$. In this form, for a randomly oriented system, it is $H = 0$; a system aligned perpendicular to the direction of diffusion will have $H = 1/2$ and a system aligned along the direction of diffusion will have $H = -1/2$. With this in mind, the expression for D_{eff} takes the form

$$\frac{D_{eff}}{D_0} = \frac{1-\varphi}{1+(H+1/2)\frac{\alpha\varphi}{2}} = \frac{1-\varphi}{1+\frac{\alpha\varphi}{2}\langle\cos^2(\theta)\rangle} \tag{10}$$

Equation (10) correctly reverts to the Nielsen model for flakes aligned normal to the direction of diffusion ($\theta = 0$) and to the dilute limit model ($D_{eff} \sim 1 - \varphi$) for flakes aligned parallel to the direction of diffusion ($\theta = \pi/2$). It should be noted that the term $(H + 1/2)$ in equation (10) is no different than the 22-diagonal component of the orientation tensor (**A**), defined as $A_{ij} = \langle p_i p_j \rangle$. Since for the two-dimensional cross sections considered in this study, $p_1 = \sin(\theta)$, $p_2 = \cos(\theta)$, it is $\mathbf{A} = \begin{vmatrix} \langle\sin^2(\theta)\rangle & \langle\sin(\theta)\cos(\theta)\rangle \\ \langle\sin(\theta)\cos(\theta)\rangle & \langle\cos^2(\theta)\rangle \end{vmatrix}$. Using a similar reasoning, Lee et al.[17] proposed to use Herman's orientation function but in the context of Cussler's model,[1] which is more suitable for dense systems; adapted to a 2D system and using (H) in the form indicated earlier, the resulting expression for D_{eff} reads

$$\frac{D_{eff}(\theta)}{D_0} = \left[1 + \frac{\alpha^2\varphi^2}{(1-\varphi)}\langle\cos^2(\theta)\rangle\right]^{-1} \tag{11}$$

Recently, Dondero et al.[7] proposed a model which also makes use of the orientational metric (H). Keeping in mind our previous discussion on the application of the Herman's orientation function in 2D and 3D systems, we write the model of Dondero et al.[7] as

$$\frac{D_{eff}}{D_0} = \frac{1-\varphi}{\left[1+\left(H+\frac{1}{2}\right)\frac{5\alpha\varphi}{9}\right]^2} = \frac{1-\varphi}{\left[1+\frac{5\alpha\varphi}{9}\langle\cos^2(\theta)\rangle\right]^2} \tag{12}$$

The ensemble average directional cosine term $\langle\cos^2(\theta)\rangle$ assumes a simple and easier to understand form, when the flakes assume equiprobable random orientations in the interval $[-\varepsilon, +\varepsilon]$. It can be shown that $H + \frac{1}{2} = \langle\cos^2(\theta)\rangle = \left(\frac{1}{2} + \frac{\sin(2\varepsilon)}{4\varepsilon}\right)$ and thus, in case of a uniform distribution of flake orientations, the model of Dondero et al.[7] can be written as

$$\frac{D_{eff}}{D_0} = \frac{1-\varphi}{\left[1+\left(1+\frac{\sin(2\varepsilon)}{2\varepsilon}\right)\frac{5\alpha\varphi}{18}\right]^2} \tag{13}$$

The predictions of equations (10), (11), and (12) are compared to the models derived in this study and to computational results in the following figures. Figure 9 shows comparisons corresponding to $\alpha = 1000$ and

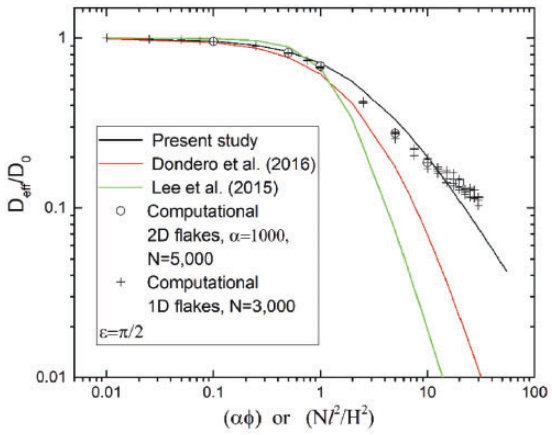

Figure 9. Comparison between computational results for 2D and 1D flakes (o,+) and the predictions of various theoretical models. The results of the current study correspond to the use of the harmonic average, equation (6).

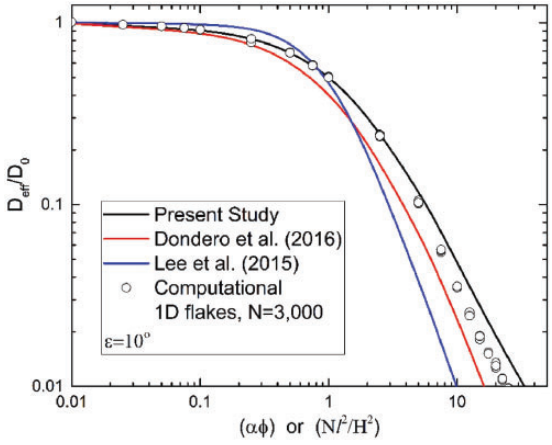

Figure 10. Comparison between computational results for 1D flakes (o) and the predictions of various theoretical models, when flakes assume random orientations in the interval $[-10^\circ, +10^\circ]$. The results of the current study shown correspond to the use of the harmonic average, equation (6).

$\varepsilon = \pi/2$. The computational results shown correspond to 2D flake representation and $N = 5000$ and also to 1D flakes and $N = 3000$. It is evident that the model proposed in this study follows the computational results more closely, up to very large values of the concentration parameter ($\alpha\varphi$). When the misalignment angle decreases, the predictions of the various models come closer together and also closer to the computational results. This is shown in Figure 10. In the case of small misalignment angles, the predictions of the models based on the harmonic, arithmetic, and geometric averages are also close to each other (e.g., Figure 6).

Conclusions

We have presented a closed-form solution for the effective diffusion coefficient of flake-filled composites, in which the flakes are randomly placed and oriented, with the orientations uniformly distributed in an interval $[-\varepsilon, +\varepsilon]$, $0 < \varepsilon < \pi/2$. Our solution is based on the harmonic averaging of the diffusivity of unidirectional misaligned flake systems, and has been extensively validated using large-scale 2D simulations. In these simulations, we have used both, traditional 2D (rectangles of finite aspect ratio) and also 1D (lines) representations of the flake cross sections. The 1D representation is suitable for very high aspect ratio flakes, such as exfoliated nano-platelets of montmorillonite or graphene oxide. This approach greatly simplifies the construction of the computational mesh. It is also feasible approach to model flake nanocomposites ($\alpha > 1000$), in which ($\alpha\varphi$) can reach levels in excess of 100. The actual aspect ratio (α) of nano-platelets is not easy to measure[15] and its value is sometimes unclear. In certain cases, values of (α) were reported based on fitting simple, and in light of the present study, inadequate, permeability models to experimental data. For example, in Roding et al.,[9] it was clear that a perfect fit between model and experiment could only be achieved if a value of (α) that was about 1/3 of the expected value was used. Our proposed solution for D_{eff} offers a better alternative in case such an indirect estimation of (α) is to be attempted. Our solution is found to be in very good agreement with computational results for all stages of misalignment (from unidirectional to random) and for ($\alpha\varphi$) up to 30 for a randomly oriented composite and higher for lower (ε). The predictions of the proposed solution were also compared to those of existing literature models. We find that discrepancies become very significant at large (ε) and also at large values of ($\alpha\varphi$), pointing further to the conclusion that the proposed solution is currently the only accurate one to predict the effective diffusivity of randomly oriented and highly concentrated nano-flake composites. There is still a degree of empiricism in our proposed solution, and this can be traced in the choice of the tortuosity parameter (λ) used in the context of the model of Lape et al.[4] for the principal diffusivity D_{11} (fully aligned system). Similar empirical coefficients can be found in the other models tested in this study, such as in equations (10)–(13). However, because of the robust foundation of our model on the properties of the diffusivity tensor and on formal averaging (e.g., equation(6)), once a value of (λ) is determined by fitting the unidirectional data, a good fit with computational results at all states of misalignment is achieved without the need for additional adjustable parameters. In other models, the corresponding geometrical factors will have to become functions of ($\alpha\varphi$) and (ε) in order for their predictions

to be reliable across the entire space of concentration and misalignment.

Declaration of Conflicting Interests

The author(s) declared no potential conflicts of interest with respect to the research, authorship, and/or publication of this article.

Funding

The author(s) received no financial support for the research, authorship, and/or publication of this article.

ORCID iD

A Tsiantis http://orcid.org/0000-0003-2955-5459

References

1. Cussler EL, Hughes SE, Ward WJ, et al. Barrier membranes. *J Membr Sci* 1988; 38: 161–174.
2. Aris R. On a problem in hindered diffusion. *Arch Rat Mech Anal* 1986; 95: 83–91.
3. Chen X and Papathanasiou TD. Barrier properties of flake-filled membranes: review and numerical evaluation. *J Plast Film Sheet* 2007; 23: 319–346.
4. Lape NK, Nuxoll EE and Cussler EL. Polydisperse flakes in barrier films. *J Membr Sci* 2004; 236: 29–37.
5. Tsiantis A and Papathanasiou TD. The barrier properties of flake-filled composites with precise control of flake orientation. *Mater Sci Appl Spec Issue Addit Manufact* 2017; 8: 234–246.
6. Papathanasiou TD and Tsiantis A. Orientational randomness and its influence on the barrier properties of flake-filled composite films. *J Plast Film Sheet* 2017; 33: 438–456.
7. Dondero M, Tomba JP and Cisilino AP. The effect of flake orientational order on the permeability of barrier membranes: numerical simulations and predictive models. *J Membr Sci* 2016; 514: 95–104.
8. Zid S, Zinet M and Espuche E. Modeling diffusion mass transport in multiphase polymer systems for gas barrier applications: a review. *Polym Sci Part B Polym Phys* 2018; 56: 621–638.
9. Roding M, Gaska K, Kadar R, et al. Computational screening of diffusive transport in nanoplatelet-filled composites: use of graphene to enhance polymer barrier properties. *ACS Appl Nano Mater* 2018; 1(1): 160–167.
10. Wolf C, Angelier-Coussy H, Contard N, et al. How the shape of fillers affects the barrier properties of polymer/non-porous particles nanocomposites: a review. *J Membr Sci* 2018; 556: 393–418.
11. Dontero M, Cisilino AP and Tomba JP. Experimental validation of computational models for mass transport through micro heterogeneous membranes. *J Membr Sci* 2013; 437: 25–32.
12. Nielsen LE. Models for the permeability of filled polymer systems. *J Macromol Sci Part A Chem* 1967; 5: 929–942.
13. Minelli M, Baschetti MG and Doghierri F. A comprehensive model for mass transport properties in nanocomposites. *J Membr Sci* 2011; 381: 10–20.
14. Lusti HR, Gusev AA and Guseva O. The influence of platelet disorientation on the barrier properties of composites: a numerical study. *Modelling Simul Mater Sci Eng* 2004; 12: 1201–1207.
15. Tan B and Thomas NL. A review of the water barrier properties of polymer/clay and polymer/graphene nanocomposites. *J Membr Sci* 2016; 514: 595–612.
16. Bharadwaj RK. Modeling the barrier properties of polymer-layered silicate nanocomposites. *Macromolecules* 2001; 34: 9189–9192.
17. Lee K-H, Hong J, Kwak SJ, et al. Spin self-assembly of highly ordered multilayers of graphene-oxide sheets for improving oxygen barrier performance in polyolefins. *Carbon* 2015; 83: 40–47.